

Photonic trimming of quantum emitters via direct fabrication of metallic nanostructures

Xin Li, Rong-Ling Su, Zhang-Kai Zhou, Ying Yu, and Andrea Di Falco

Citation: *APL Photonics* **3**, 071301 (2018); doi: 10.1063/1.5034314

View online: <https://doi.org/10.1063/1.5034314>

View Table of Contents: <http://aip.scitation.org/toc/app/3/7>

Published by the [American Institute of Physics](#)

AIP | Conference Proceedings

Get **30% off** all
print proceedings!

Enter Promotion Code **PDF30** at checkout



Photonic trimming of quantum emitters via direct fabrication of metallic nanostructures

Xin Li,¹ Rong-Ling Su,^{2,3} Zhang-Kai Zhou,^{2,3} Ying Yu,^{2,4}
 and Andrea Di Falco^{1,a}

¹*SUPA, School of Physics and Astronomy, University of St Andrews, North Haugh,
 St Andrews KY16 9SS, United Kingdom*

²*State Key Laboratory of Optoelectronic Materials and Technologies, Sun Yat-Sen University,
 Guangzhou 510275, People's Republic of China*

³*School of Physics, Sun Yat-Sen University, Guangzhou 510275, People's Republic of China*

⁴*School of Electronics and Information Technology, Sun Yat-Sen University,
 Guangzhou 510275, People's Republic of China*

(Received 10 April 2018; accepted 25 May 2018; published online 15 June 2018)

In this paper, we demonstrate the control of the emission of a GaAs quantum dot embedded in a GaAs/AlGaAs nanowire by the post-fabrication of a plasmonic grating on its surface. Using a direct electron beam-induced deposition of Pt nanowires, we demonstrate an enhancement of the emission efficiency for the polarization parallel to the nanowires of 45%, with a 17% reduction in the photon lifetime. We believe that these results will help establish a new hybrid nanophotonic platform for efficient single photon sources. © 2018 Author(s). All article content, except where otherwise noted, is licensed under a Creative Commons Attribution (CC BY) license (<http://creativecommons.org/licenses/by/4.0/>). <https://doi.org/10.1063/1.5034314>

I. INTRODUCTION

Semiconductor quantum dots (QDs) are excellent candidates for quantum light emitters at the single photon level because of their stability, narrow spectral linewidth, and short radiative lifetime.^{1,2} By engineering the photonic environment of the QDs, it is possible to condition their emission, coupling photons into different nanostructures with controlled lifetimes and high internal and external quantum efficiency.^{2–8} The key requirements for the realization of efficient single photon emitters are a high quality factor of the photonic cavity and a low modal spatial volume, required to minimize the emission threshold and increase the efficiency. Besides, a short lifetime is desirable to increase the emission efficiency and for high modulation speed.

Dielectric resonators, such as photonic crystal cavities, micropillars, and microdisks, are typically favored for the high quality factor achievable, at the cost of relatively large modal volumes and long photon lifetimes.^{2,9–14} Recently the case has been made for single photon quantum emitters based on plasmonic nanoresonators, which guarantee drastically reduced volumes and photon lifetimes, at the cost of high absorption losses and low quality factors.^{3,15,16} Independent of the platform of choice, there is clear evidence that the definition of controlled advanced photonic environment is the most promising route to achieve efficient single photon emission. To this end, a common practical technological issue to overcome is the stringent positioning of the QDs in the engineered photonic landscape. This has been solved with a number of techniques, including the use of atomic force microscopes (AFMs)^{17–19} or photolithographic techniques^{20,21} to locate and mark the QD position, the post-fabrication positioning of plasmonic nanoparticles in proximity to randomly located QD,^{22,23} and the realization of polymeric waveguides around the QD dispersed in bulk polymers.^{24,25}

A different approach is based on the post-fabrication modification of the photonic response of the microcavities hosting the QDs, in order to control the properties of the emitted photons, as

^aAuthor to whom correspondence should be addressed: adf10@st-andrews.ac.uk

for example possible with hot-tip lithographic patterning.²⁶ Here we propose a new technological platform based on the photonic trimming of semiconductor nanowires (NWs) embedding QDs,^{27–29} via the direct electron beam-induced deposition (EBID)^{30–32} of plasmonic features. This approach conjugates the quality of the semiconductor NWs with the flexibility of design of the plasmonic platform and the relaxation of the alignment requirements since the QD cannot be located before embedding it in a conveniently shaped resonator. Specifically, in this work, we use the EBID method to design and create a sub-wavelength Pt grating on a core-shell GaAs/AlGaAs NW that contains GaAs QDs.

By introducing a Pt grating structure above the QDs, we demonstrate the modification of polarization of QD emission, with an increase in the emission efficiency and an associated reduction in the QD radiative lifetime.

II. FABRICATION

The core-shell GaAs/AlGaAs NWs hosting GaAs QDs were fabricated on GaAs (001) substrate via molecular beam epitaxy (MBE),¹⁶ as sketched in Fig. 1(a). The GaAs substrate was sputter-coated with a 15 nm silicon dioxide layer and dipped in 10% HF aqueous solution for 2 s to create randomly distributed vacancy spots for the growth of the NWs. The substrate was then loaded into the MBE system, and the vacancy spots were covered with 1 nm size Ga droplets, to start the vertical growing of GaAs cores. As soon as the NW reached the designed length of 3.5 μm , the vertical growth was interrupted by the deposition of a second Ga droplet, which triggered the lateral growth. When the width of GaAs NW reached 200 nm, the other two Al_{0.7}Ga_{0.3}As barrier shells with thickness of 200 nm were fabricated to cover the GaAs core, and the GaAs QDs grew between them, laterally on the facet of the NWs. In the end, the core-shell GaAs/Al_{0.7}Ga_{0.3}As NWs embedded with GaAs QDs were coated with another 60-nm thick GaAs layer to protect the QDs. This procedure typically yields to NWs hosting one single QD.^{28,33} While this is a critical condition for single photon emission, the validity of our proof-of-principle demonstration goes beyond this regime.

After the MBE process, the NWs embedded with QDs were detached from the GaAs substrate onto a target substrate by a simple contact transfer. In order to simplify the deterministic location and measurement of individual NWs, we used as target a silicon substrate coated with SiO₂, marked with back-etched, numbered Au frames. After a preliminary characterization, selected NWs were patterned with sub-wavelength Pt gratings, using the EBID.

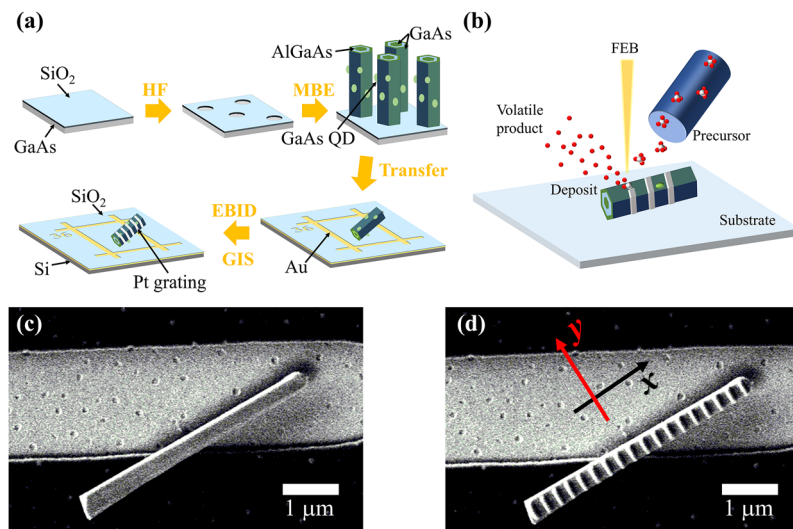


FIG. 1. (a) Fabrication processes of GaAs/AlGaAs NWs, GaAs QDs, and Pt grating. (b) Deposition diagram of the EBID method. (c) The scanning electron microscope (SEM) image of a GaAs/AlGaAs NW on SiO₂/Au substrate. (d) The SEM image of the Pt grating on the NW shown in (c).

For this purpose, we used a Raith E-line plus electron beam lithographic system, as shown in Fig. 1(b). The EBID approach permits to deposit selected materials with nanometric positional accuracy, reducing with a focused electron beam (FEB) specific gas precursors, injected in the chamber in proximity of the target.^{30,32,34} To deposit Pt, a suitable precursor is a compound based on $(\text{Me}_3)\text{MeCpPt}$. The resulting deposited material consists mostly of Pt atoms in a carbon matrix, with dilution percentage that varies from 10% to up to 100% Pt, depending on the specific deposition parameters and post-fabrication procedures.³⁵ In our case, we used a deposition current of 150 pA, acceleration voltage of 3 kV, and dose of 1 C/cm², at room temperature, which leads to an expected Pt percentage of 30%.³⁶ While the choice of the Pt was dictated by the precursor availability, this is a simple limitation of our instrument and not of the technique. For example, suitable precursors to deposit gold are also available, e.g., in ion beam-induced deposition systems.^{37,38}

Figures 1(c) and 1(d) show scanning electron microscope (SEM) pictures of the NW before and after the deposition of the Pt grating, respectively. The grating was composed of wires of 50 nm width, 250 nm period, and 100 nm thickness. To design the grating, we approximated the optical mode in the NW with a guided mode with an effective index of $n = 3.6$.^{28,39} As visible from Fig. 1(d), the metallic pattern was perfectly aligned with the NW and only covering its top surface. The SEM pictures clearly show that the NW is suspended over a silica trench on the substrate. Given the refractive index contrast between the NW and the substrate (and/or air), we exclude that the emission dynamics is influenced significantly by this configuration. Additionally, in the following, we compare directly the emission of the QDs on the bare and patterned NW, without modifying the position of the wire respect to the alignment feature, thus canceling any potential minor contribution from the uneven substrate.

III. RESULTS AND DISCUSSION

The emission of the NWs was measured using a micro-photoluminescence (PL) imaging method,^{40–42} with the setup sketched in Fig. 2. The sample was mounted on a motorized positioning system and placed in an optical microscopy cryostat (Montana) at cryogenic temperatures as low as 3.4 K. Before (bare) and after (dressed) the fabrication of the Pt grating, the QDs in the selected NW

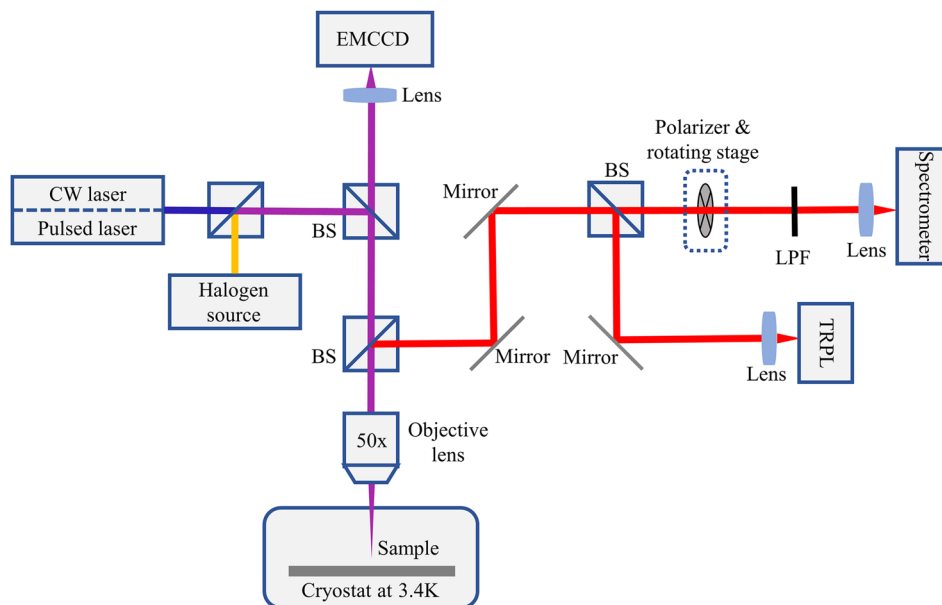


FIG. 2. The diagram of micro-PL measurement optical path, formed by pump sources (CW laser or pulsed source), illumination source (halogen source), light-matter interaction platform (cryostat), sample position locating path (EMCCD), PL spectrum analyzing path (spectrometer), photon lifetime detecting path (TRPL), etc.

were pumped with a focused continuous-wave (CW) laser beam or a 800 fs pulsed laser (80 MHz) with wavelengths of 405 nm and 780 nm, respectively. To illuminate the sample and locate the NW of interest, we added a low-power halogen source to the path of the focused laser beam. The upper arm of the setup collected the reflected light (pump and illumination component) and the light emitted by the QDs and routed it with two beam splitters (BSs) toward three distinct measurement arms. The first arm was imaged by an Electron Multiplied Charge Coupled Device (EMCCD) to locate the position of the NWs and QDs. The second path was used when the QDs were pumped with CW laser. This path was analyzed with a spectrometer and included a rotating polarizer and a 495 nm long-pass filter (LPF), to determine the emission wavelength and polarization state of the QDs, while cutting the pump wavelength. When using the pulsed laser as a pump source, the third light path was analyzed with a time-resolved photoluminescence (TRPL) system, to measure the photon lifetime of the QDs.⁴²

The NW of Figs. 1(c) and 1(d) was measured before and after the definition of the grating in nominally identical experimental conditions and at the same pump power (20 μW). The top and bottom panels in Fig. 3(a) show the emission spectra of the bare and dressed NWs, respectively, without the output polarizer. From a first analysis, it emerges that the emission wavelength of the (single) QD embedded in the NW around 674 nm does not shift after the deposition of the Pt nanostructures. Conversely, the presence of the metallic grating appears to decrease the emission intensity by slightly more than 75%. Additionally, the dressed NW shows a 17% reduction in photon lifetime compared to the bare NW, as visible in Fig. 3(b). The inset of Fig. 3(b) shows the collected intensity for different pump powers for the bare and dressed NWs. The fact that the two curves have a similar gradient in the 20 μW region permits us to compare directly the lifetimes of the NW in the two different regimes of efficiency. From these measurements alone, it is not straightforward to estimate whether the reduction in the lifetime is due to a radiative or non-radiative contribution^{6,8} since the grating is expected to introduce absorption losses but also to increase the overall efficiency.

To address in more details the coupling dynamics between the emission mode supported by the NW and the grating, we placed a linear polarizer in the optical path (see Fig. 2). The panels in Fig. 3(c) indicate a marked difference in the polarization state of the emitted radiation, due to the presence of the grating. Whereas the bare NW mostly emits with polarization perpendicular to its long axis, the dressed NW emits photons mostly polarized along the long axis. This result can be explained noting that the QDs grown on the surface of these type of NWs can be approximated by dipoles oscillating perpendicularly to the long axis,^{28,33} which couple to one of the photonic modes of the high refractive index NW. The presence of the grating suppresses drastically the component oscillating along the Pt wires (y direction), whereas it improves the out-coupling of the transverse component

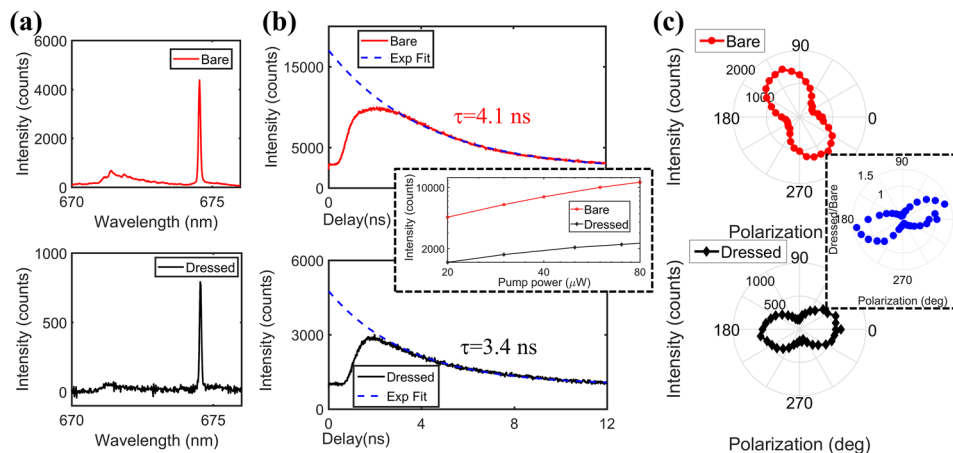


FIG. 3. Measurement results of QD emission intensity, radiative lifetime, and polarization states of bare and dressed NWs. (a) Emitting spectra of bare and dressed NWs without the polarizer before spectrometer. (b) Emission intensity vs. pump power (dash frame) and different radiative lifetimes (τ) of bare and dressed NWs. (c) Emission polarization state results of bare and dressed NWs attached with the intensity ratio between dressed and bare NW in different polarization states.

(x direction), with an associated reduction in the photon lifetime. This is quantitatively demonstrated by plotting the ratio of the emission intensity of the dressed and bare NWs, which shows a maximum enhancement of the collected emission in the order of 45%, along the x direction.

In this proof-of-principle demonstration of a hybrid nanophotonic quantum platform, the coupling between the NW and the grating was designed on the basis of a number of assumptions, supported by a simplified model of the NW²⁸ and by a direct comparison of the emission properties of the NW before and after the fabrication of the plasmonic grating. Recent studies on the full QD/NW system show that the emission efficiency depends strongly on the specific position of the QD in the NW and on the orientation of the NW on the substrate.²⁸ We expect that tailoring the plasmonic nanostructure to the position of the QDs can lead to a dramatic further enhancement of the emission, with controlled polarization of the emitted state.

The specific electromagnetic field of a lasing NW can be directly acquired with near-field microscopy, e.g., using an AFM¹⁹ or via cathodoluminescence,²⁸ or indirectly, e.g., measuring the emission efficiency. Importantly, these methods can be automated⁴³ and integrated in the workflow process, to scale up the technique. In a typical procedure, the alignment markers in the substrate will be used to map the distribution of the NWs which, after the topological or photonic characterization, will be decorated with the most suitable plasmonic structures, chosen within a library of available geometries. Both the alignment accuracy and the deposition time are typical of nanolithographic processes; hence, it is expected that the throughput will be comparable with modern fabrication techniques.

We anticipate that this fabrication approach, based on the post-fabrication and alignment-free photonic trimming of quantum emitters, will enable a new platform of quantum sources at the single photon level.

IV. CONCLUSION

In this letter, we demonstrated that the EBID technology can be used to effectively modify the photonic response of a quantum emitter embedded in a semiconductor NW, by depositing a suitable nanopattern on its surface, without requiring additional wet lithographic steps. In particular, we demonstrated that adding a subwavelength grating of Pt on the top side of a NW hosting a semiconductor QD permits us to control the polarization of the emitted light, with an overall reduction in the lifetime of 17% and an increase in the collection efficiency up to 45%, for the polarization parallel to the NW. We argue that applying the EBID method to QD emitters opens the door to the realization of new efficient quantum sources at the single photon level.

ACKNOWLEDGMENTS

A.D.F. and Z.Z.K. acknowledge support from the Royal Society (No. IE141537). The grant was also supported by ESPRC (No. EP/L017008/1), the National Natural Science Foundation of China (Nos. 61675237 and 11704424), the Guangdong Natural Science Foundation (No. 2017B030306007), and the Guangzhou Science and Technology Projects (No. 201806010033). The research data supporting this publication can be accessed at <http://dx.doi.org/10.17630/7c40980c-8911-4837-8d51-b4d547014de1>.

¹ P. Michler, A. Kiraz, C. Becher, W. Schoenfeld, P. Petroff, L. Zhang, E. Hu, and A. Imamoglu, "A quantum dot single-photon turnstile device," *Science* **290**(5500), 2282–2285 (2000).

² J. P. Reithmaier, "Strong exciton–photon coupling in semiconductor quantum dot systems," *Semicond. Sci. Technol.* **23**(12), 123001 (2008).

³ T. B. Hoang, G. M. Akselrod, and M. H. Mikkelsen, "Ultrafast room-temperature single photon emission from quantum dots coupled to plasmonic nanocavities," *Nano Lett.* **16**(1), 270–275 (2015).

⁴ I. Söllner, S. Mahmoodian, S. L. Hansen, L. Midolo, A. Javadi, G. Kiršanskė, T. Pregolato, H. El-Ella, E. H. Lee, and J. D. Song, "Deterministic photon–emitter coupling in chiral photonic circuits," *Nat. Nanotechnol.* **10**(9), 775 (2015).

⁵ R. Chikkaraddy, B. De Nijs, F. Benz, S. J. Barrow, O. A. Scherman, E. Rosta, A. Demetriadou, P. Fox, O. Hess, and J. J. Baumberg, "Single-molecule strong coupling at room temperature in plasmonic nanocavities," *Nature* **535**(7610), 127 (2016).

⁶ M. Pfeiffer, K. Lindfors, P. Atkinson, A. Rastelli, O. G. Schmidt, H. Giessen, and M. Lippitz, "Positioning plasmonic nanostructures on single quantum emitters," *Phys. Status Solidi B* **249**(4), 678–686 (2012).

- ⁷ Y. Gu, L. Huang, O. J. Martin, and Q. Gong, "Resonance fluorescence of single molecules assisted by a plasmonic structure," *Phys. Rev. B* **81**(19), 193103 (2010).
- ⁸ P. Anger, P. Bharadwaj, and L. Novotny, "Enhancement and quenching of single-molecule fluorescence," *Phys. Rev. Lett.* **96**(11), 113002 (2006).
- ⁹ J. Reithmaier, G. Şek, A. Löffler, C. Hofmann, S. Kuhn, S. Reitzenstein, L. Keldysh, V. Kulakovskii, T. Reinecke, and A. Forchel, "Strong coupling in a single quantum dot–semiconductor microcavity system," *Nature* **432**(7014), 197 (2004).
- ¹⁰ E. Peter, P. Senellart, D. Martrou, A. Lemaître, J. Hours, J. Gérard, and J. Bloch, "Exciton-photon strong-coupling regime for a single quantum dot embedded in a microcavity," *Phys. Rev. Lett.* **95**(6), 067401 (2005).
- ¹¹ J. Gérard, B. Sermage, B. Gayral, B. Legrand, E. Costard, and V. Thierry-Mieg, "Enhanced spontaneous emission by quantum boxes in a monolithic optical microcavity," *Phys. Rev. Lett.* **81**(5), 1110 (1998).
- ¹² O. Benson, C. Santori, M. Pelton, and Y. Yamamoto, "Regulated and entangled photons from a single quantum dot," *Phys. Rev. Lett.* **84**(11), 2513 (2000).
- ¹³ A. Löffler, J. Reithmaier, G. Şek, C. Hofmann, S. Reitzenstein, M. Kamp, and A. Forchel, "Semiconductor quantum dot microcavity pillars with high-quality factors and enlarged dot dimensions," *Appl. Phys. Lett.* **86**(11), 111105 (2005).
- ¹⁴ D. Press, S. Götzinger, S. Reitzenstein, C. Hofmann, A. Löffler, M. Kamp, A. Forchel, and Y. Yamamoto, "Photon antibunching from a single quantum-dot-microcavity system in the strong coupling regime," *Phys. Rev. Lett.* **98**(11), 117402 (2007).
- ¹⁵ M. S. Tame, K. McEnery, Ş. Özdemir, J. Lee, S. Maier, and M. Kim, "Quantum plasmonics," *Nat. Phys.* **9**(6), 329 (2013).
- ¹⁶ S. I. Bozhevolnyi and N. A. Mortensen, "Plasmonics for emerging quantum technologies," *Nanophotonics* **6**(5), 1185–1188 (2017).
- ¹⁷ R. Stomp, Y. Miyahara, S. Schaer, Q. Sun, H. Guo, P. Grutter, S. Studenikin, P. Poole, and A. Sachrajda, "Detection of single-electron charging in an individual InAs quantum dot by noncontact atomic-force microscopy," *Phys. Rev. Lett.* **94**(5), 056802 (2005).
- ¹⁸ J. F. Campbell, I. Tessmer, H. H. Thorp, and D. A. Eerie, "Atomic force microscopy studies of DNA-wrapped carbon nanotube structure and binding to quantum dots," *J. Am. Chem. Soc.* **130**(32), 10648–10655 (2008).
- ¹⁹ L. Sapienza, J. Liu, J. D. Song, S. Fält, W. Wegscheider, A. Badolato, and K. Srinivasan, "Combined atomic force microscopy and photoluminescence imaging to select single InAs/GaAs quantum dots for quantum photonic devices," *Sci. Rep.* **7**(1), 6205 (2017).
- ²⁰ P. Pompa, L. Martiradonna, A. Della Torre, F. Della Sala, L. Manna, M. De Vittorio, F. Calabi, R. Cingolani, and R. Rinaldi, "Metal-enhanced fluorescence of colloidal nanocrystals with nanoscale control," *Nat. Nanotechnol.* **1**(2), 126 (2006).
- ²¹ J.-H. Song, T. Atay, S. Shi, H. Urabe, and A. V. Nurmikko, "Large enhancement of fluorescence efficiency from CdSe/ZnS quantum dots induced by resonant coupling to spatially controlled surface plasmons," *Nano Lett.* **5**(8), 1557–1561 (2005).
- ²² Y.-P. Hsieh, C.-T. Liang, Y.-F. Chen, C.-W. Lai, and P.-T. Chou, "Mechanism of giant enhancement of light emission from Au/CdSe nanocomposites," *Nanotechnology* **18**(41), 415707 (2007).
- ²³ O. Kulakovich, N. Strelak, A. Yaroshevich, S. Maskevich, S. Gaponenko, I. Nabiev, U. Woggon, and M. Artemyev, "Enhanced luminescence of CdSe quantum dots on gold colloids," *Nano Lett.* **2**(12), 1449–1452 (2002).
- ²⁴ A. W. Schell, H. Takashima, T. T. Tran, I. Aharonovich, and S. Takeuchi, "Coupling quantum emitters in 2D materials with tapered fibers," *ACS Photonics* **4**(4), 761–767 (2017).
- ²⁵ S. Strauf, N. G. Stoltz, M. T. Rakher, L. A. Coldren, P. M. Petroff, and D. Bouwmeester, "High-frequency single-photon source with polarization control," *Nat. Photonics* **1**(12), 704 (2007).
- ²⁶ D. Pires, J. L. Hedrick, A. De Silva, J. Frommer, B. Gotsmann, H. Wolf, M. Despont, U. Duerig, and A. W. Knoll, "Nanoscale three-dimensional patterning of molecular resists by scanning probes," *Science* **328**(5979), 732–735 (2010).
- ²⁷ H. J. Fan, P. Werner, and M. Zacharias, "Semiconductor nanowires: From self-organization to patterned growth," *Small* **2**(6), 700–717 (2006).
- ²⁸ Y. Yu, X. M. Dou, B. Wei, G. W. Zha, X. J. Shang, L. Wang, D. Su, J. X. Xu, H. Y. Wang, and H. Q. Ni, "Self-assembled quantum dot structures in a hexagonal nanowire for quantum photonics," *Adv. Mater.* **26**(17), 2710–2717 (2014).
- ²⁹ J. Claudon, J. Bleuse, N. S. Malik, M. Bazin, P. Jaffrennou, N. Gregersen, C. Sauvan, P. Lalanne, and J.-M. Gérard, "A highly efficient single-photon source based on a quantum dot in a photonic nanowire," *Nat. Photonics* **4**(3), 174 (2010).
- ³⁰ H. W. Koops, J. Kretz, M. Rudolph, M. Weber, G. Dahm, and K. L. Lee, "Characterization and application of materials grown by electron-beam-induced deposition," *Jpn. J. Appl. Phys., Part 1* **33**(12S), 7099 (1994).
- ³¹ W. F. Van Dorp, B. Van Someren, C. W. Hagen, P. Kruit, and P. A. Crozier, "Approaching the resolution limit of nanometer-scale electron beam-induced deposition," *Nano Lett.* **5**(7), 1303–1307 (2005).
- ³² F. De Angelis, C. Liberale, M. Coluccio, G. Cojoc, and E. Di Fabrizio, "Emerging fabrication techniques for 3D nanostructuring in plasmonics and single molecule studies," *Nanoscale* **3**(7), 2689–2696 (2011).
- ³³ M. Heiss, Y. Fontana, A. Gustafsson, G. Wüst, C. Magen, D. O'regan, J. Luo, B. Ketterer, S. Conesa-Boj, and A. Kuhlmann, "Self-assembled quantum dots in a nanowire system for quantum photonics," *Nature Mater.* **12**(5), 439 (2013).
- ³⁴ W. Van Dorp and C. W. Hagen, "A critical literature review of focused electron beam induced deposition," *J. Appl. Phys.* **104**(8), 081301 (2008).
- ³⁵ M. Esposito, V. Tasco, M. Cuscuna, F. Todisco, A. Benedetti, I. Tarantini, M. D. Giorgi, D. Sanvitto, and A. Passaseo, "Nanoscale 3D chiral plasmonic helices with circular dichroism at visible frequencies," *ACS Photonics* **2**, 105–114 (2014).
- ³⁶ S. Frabboni, G. Gazzadi, L. Felisari, and A. Spessot, "Fabrication by electron beam induced deposition and transmission electron microscopic characterization of sub-10-nm freestanding Pt nanowires," *Appl. Phys. Lett.* **88**(21), 213116 (2006).
- ³⁷ G. Seniutinas, A. Balčytis, I. Reklaitis, F. Chen, J. Davis, C. David, and S. Juodkazis, "Tipping solutions: Emerging 3D nano-fabrication/-imaging technologies," *Nanophotonics* **6**(5), 923–941 (2017).
- ³⁸ V. Tasco, M. Esposito, F. Todisco, A. Benedetti, M. Cuscuna, D. Sanvitto, and A. Passaseo, "Three-dimensional nanohelices for chiral photonics," *Appl. Phys. A* **122**(4), 280 (2016).
- ³⁹ R. Yan, D. Gargas, and P. Yang, "Nanowire photonics," *Nat. Photonics* **3**(10), 569 (2009).

- ⁴⁰ J. Wang, Y. Yu, Y.-M. Wei, S.-F. Liu, J. Li, Z.-K. Zhou, Z.-C. Niu, S.-Y. Yu, and X.-H. Wang, "High-efficiency broadband second harmonic generation in single hexagonal GaAs nanowire," *Sci. Rep.* **7**(1), 2166 (2017).
- ⁴¹ S. Cao, X. Ji, K. Qiu, Y. Gao, Y. Zhao, J. Tang, Z. Xu, K. Jin, and X. Xu, "Resolving exciton diffusion in InGaAs quantum wells using micro-photoluminescence mapping with a lateral excitation," *Semicond. Sci. Technol.* **28**(12), 125004 (2013).
- ⁴² S. Liu, Y. Wei, R. Su, R. Su, B. Ma, Z. Chen, H. Ni, Z. Niu, Y. Yu, and Y. Wei, "A deterministic quantum dot micropillar single photon source with >65% extraction efficiency based on fluorescence imaging method," *Sci. Rep.* **7**(1), 13986 (2017).
- ⁴³ J. A. Alanis, D. Saxena, S. Mokkalapati, N. Jiang, K. Peng, X. Tang, L. Fu, H. H. Tan, C. Jagadish, and P. Parkinson, "Large-scale statistics for threshold optimization of optically pumped nanowire lasers," *Nano Lett.* **17**(8), 4860–4865 (2017).